

Chinese Journal of Oceanology and Limnology  
 Vol. 27 No. 1, P. 112-116, 2009  
 DOI: 10.1007/s00343-009-0112-1

# A new model to estimate significant wave heights with ERS-1/2 scatterometer data\*

GUO Jie (过杰)<sup>†, ‡, \*\*</sup>, HE Yijun (何宜军)<sup>†</sup>, William Perrie<sup>†††</sup>, SHEN Hui (申辉)<sup>†</sup>, CHU Xiaoqing (储小青)<sup>†, ‡†</sup>

<sup>†</sup>Institute of Oceanology, Chinese Academy of Sciences, Key Laboratory of Ocean Circulation and Wave, CAS, Qingdao 266071, China

<sup>‡†</sup>Graduate School of the Chinese Academy of Sciences, Beijing 100039, China

<sup>†††</sup>Bedford Institute of Oceanography, Dartmouth, NS, Canada

Received Oct. 10, 2008; revision accepted Nov. 17, 2008

**Abstract** A new model is proposed to estimate the significant wave heights with ERS-1/2 scatterometer data. The results show that the relationship between wave parameters and radar backscattering cross section is similar to that between wind and the radar backscattering cross section. Therefore, the relationship between significant wave height and the radar backscattering cross section is established with a neural network algorithm, which is, if the average wave period is  $\leq 7$ s, the root mean square of significant wave height retrieved from ERS-1/2 data is 0.51 m, or 0.72 m if it is  $> 7$ s otherwise.

**Keyword:** scatterometer; significant wave height; neural networks; wind waves; swell

## 1 INTRODUCTION

A good description of ocean wave conditions is crucial to the safety of voyage as well as of marine constructions. Ocean waves can be described with the parameters such as significant wave height, wave period, and wave direction etc. In the past, ocean wave parameters are measured with wave gauges and buoys; however, it is almost not possible for the detail and constant measurement operations at sea in a large marine area or global oceans. This situation remains unchanged until oceanic satellites were launched.

At present, synthetic aperture radar (SAR) mounted in a satellite is the only sensor used to remotely measure ocean wave spectra. However, because of the azimuthal wave cutoff and the lack of power, it is unable to measure the high-frequency part of a wave spectrum. The application is therefore limited. On the other hand, significant wave height ( $H_{1/3}$ ) can be measured globally with such a satellite radar altimeter by inferring directly from the shape of radar pulse returning to the nadir-looking altimeter with the assumption of the Gaussian surface elevations. Moreover, wind speed can also be retrieved from the altimeter-measured normalized radar cross section (NRCS). Hwang et al. (1998) established the relation among wind speed, period

and  $H_{1/3}$  with the buoys in the Gulf of Mexico, estimating the wave periods from wind speeds and altimeter-measured  $H_{1/3}$ . These wave parameters can be measured at 7 km resolution along the track. However, the two-dimensional spatial resolution quite low; therefore, its applications have been limited.

A scatterometer is a specialized sensor for measuring sea surface wind vector in spatial resolution of 50 km or less, and the precision of wind speed is about 2 m/s. As QuikSCAT can cover 90% of the global oceans every day, the data have been applied widely. The wind vector can be measured by a scatterometer because the NRCS is wind-vector dependent. In fact, the NRCS represents the radar return intensity at sea surface forced by wind. Ocean waves almost always include wind waves and swell. Therefore, the NRCS depends not only on wind vectors, but also on ocean waves. For TRMM (tropical rainfall mapping mission), the NRCS depends on the waves and wind speed, having one precipitation radar (PR) and two satellite altimeters (Jason-1 and ENVISAT) installed (Tran et al., 2007). The spectrum model by Stephen et al. (1985) is used

\* Supported by the National High Technology Research and Development Program of China (863 Program) (No.2008AA09Z102), and by the Canadian Space Agency (CSA) GRIP Program.

\*\* Corresponding author: guo\_jie8@sina.com

at ocean surface, in which two-scale scattering theory is applied, and can well predict the observed dependence of NRCS on radar frequency, polarization, incidence angle, and wind velocity in a wide incidence angle range of  $0^\circ$ – $70^\circ$ . The spectrum model is integrated with swell effect examination on a radar cross section. The effect is significant in low radar frequency (L band) at normal incidence, and can be nearly eliminated in high frequency (Ku band) at a large angle of incidence (about  $50^\circ$ ). With neural networks and large high-quality collocated datasets, Quilfen and Chapron (2003) studied the relation between the C-band scatterometer NRCS measurement by ERS (European Remote Sensing Satellite) and integrated sea state parameters (i.e., the mean wave period and significant wave height) measured by buoys, and found that the NRCS is affected by wave parameters. In the following sections, our methodology, results, and conclusions to retrieve wave parameters from ERS-1/2 scatterometer data are presented.

## 2 METHODS AND RESULTS

### 2.1 Data

The ERS missions consist of two remote sensing satellites launched in the 1990s by the European Space Agency. The first series, ERS-1, was launched in July 1991, and ERS-2 in April 1995 in order to ensure long term continuity of data, which is essential for researches and applications. ERS-1/2 (ERS-1 and ERS-2 in short) scatterometer data are used in this paper.

Because National Data Buoy Center (NDBC) buoy collects wave data hourly, for each ERS-1/2 scatterometer data point, any two buoy data points before and after the ERS-1/2 scatterometer time are selected for comparison. The wave data from NDBC buoys are acquired and reported hourly.  $H_{1/3}$ , the significant wave height (in meter) is the  $1/3$  of the highest waves during the 20 min sampling period, and the average wave period ( $T$ , in second) is the  $H_{1/3}$  that observed during the same period. The wind direction is the degrees clockwise off the true geographical North. The significant wave height and average wave period are derived from the buoy heave motion spectrum measured over a 20-min acquisition period starting at 30 min after the hour. The wind and wind direction data are collected with a wind sensor located on the buoy's mast. The elevation of the wind sensor is 5 m or 10 m above sea level. In this research, data from 34 NDBC buoys are collected; however,

data of only 12 NDBC buoys can be used (Fig.1). They covered the North Pacific Ocean and the North Atlantic Ocean. The distances of buoys to coastal regions are over 50 km. Table 1 lists the property of the data set, including the buoy station number, coordinates, water depth, and the number of data point in each data set. In total, 10 485 data from ERS-1/2 scatterometer are collocated with the NDBC buoy data in this study, of which 5 300 are used to build the model and 5 185 data are used for validation.

The NRCS ( $\sigma$ ), azimuth angles ( $\phi$ ), and incidence angles ( $\theta$ ) are measured by the ERS-1/2 scatterometer. The wind directions ( $\Phi$ ), wind speed ( $V$ ), average wave periods ( $T$ ), and significant wave heights ( $H_{1/3}$ ) are measured in NDBC buoy stations. The comparison period spans from January 1991 to December 2000. For comparisons between scatterometer and buoy data, the maximum differences in longitude is  $0.15^\circ$ ,  $0.15^\circ$  in latitude, and 0.5 h in time.

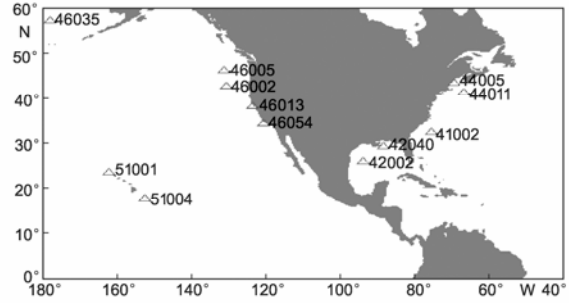


**Fig.1** Locations (triangles) of 12 buoys in the North Pacific Ocean and the North Atlantic Ocean

### 2.2 The effect of ocean wave on the radar scattering cross section

For the TRMM PR (active), Tran et al. (2007) discussed the effect of  $H_{1/3}$  on NRCS. Their results are consistent with a previous analysis at higher incidence angles ( $20^\circ$ ,  $30^\circ$ ,  $40^\circ$  and  $60^\circ$ ) (Nghiem et al., 1995). Here, ERS-1/2 scatterometer data are used with NDBC buoy data to determine the relation between wave parameters and the NRCS. Fig.2 shows the relationship between the NRCS and relative azimuth angle at an incidence angle of  $30^\circ$  when  $H_{1/3}/(gT^2)$  is 0.005. Fig.3 shows the NRCS versus relative azimuth angle curve with an incidence angle of  $45^\circ$  when  $H_{1/3}$  is 2 m. The relationship is close to that between NRCS and wind. The blue asterisks are the results from our model and the red dots represent the buoy and scatterometer observations (Figs.2 and 3).

**Table 1** Buoys data and the data collocated with ERS-1/2 scatterometer data in the Pacific and Atlantic Oceans (1991–2000)

Station	Location	Water depth (m)	Number of data points
<b>The Pacific</b>			
46002	42°35'58"N, 130°16' 19"W	3 374	67
46005	46°03'N, 131°01'12"W	2 779.8	642
46035	57°03'02"N, 177°34'35"W	3 662.3	140
51001	23°25'55"N, 162°12' 28"W	3 252	866
51004	17°31'21"N, 152°28'51"W	5 303.5	340
46054	34°16'08"N, 120°26'54"W	447.1	12
46013	38°13'30"N, 123°19'00"W	126.5	6
<b>The Atlantic</b>			
41002	32°19'08"N, 75°21'36"W	3 316.2	843
44011	41°06' 41"N, 66°34'47"W	88.4	143
44005	43°11'12"N, 69°09'48"W	195.7	642
42002	25°10'N, 94°25'00"W	3566.16	46
42040	29°11'03"N, 88° 12'48"W	443.6	123

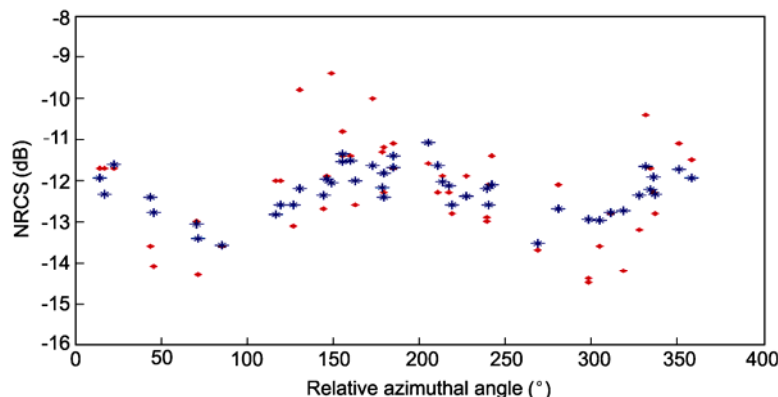


Fig.2 Relationship between relative azimuth angle and NRCS for incidence angle 30° when  $H_{1/3}/(gT^2)$  is 0.005

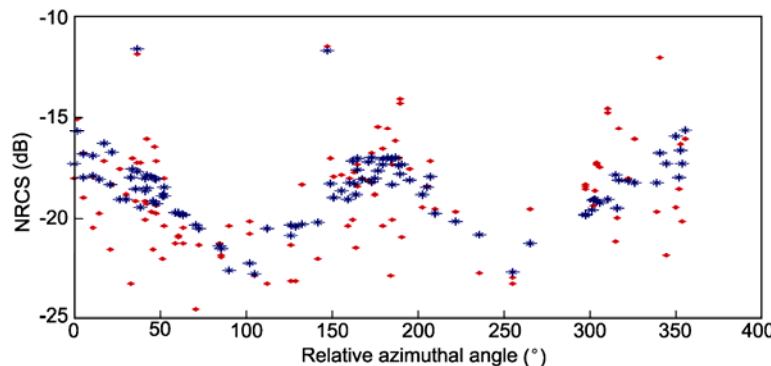


Fig.3 Relationship between relative azimuth angle and NRCS for incidence angle 45° when the  $H_{1/3}$  is 2 m

### 2.3 The algorithm of deriving ocean wave parameters

The significant wave height ( $H_{1/3}$ ) and  $H_{1/3}/(gT^2)$  are retrieved by ERS-1/2 scatterometer data using a neural network (NN) algorithm.

NN offer interesting possibilities for solving problems involved in transfer functions. First, the NN are adaptive, providing a flexible and easy way

of modeling a large variety of physical phenomena. Here, *adaptive* means the method is able to process a large number of data or deal with new relevant variables. Second, even if the learning phase of the network takes a long times, the operational phase is very efficient. This phase requires few calculations and can be performed with personal computers. Moreover, NN architecture can be easily implemented on dedicated hardware using parallel

algorithms, and further saving the processing time.

In this paper,  $H_{1/3}$  is retrieved from scatterometer data using neural networks technology.

The learning data include incidence angles ( $\theta$ ),  $\cos(\Phi-\varphi)$ , NRCS ( $\sigma$ ), wind speed (V) and  $H_{1/3}$  from buoys. The module structure consists of a multi-layer perception (MLP) that includes one hidden layers. The transfer function of the input hidden layer is a sigmoid function  $f(x)=2/[1+\exp(-2x)]$ , and that of the output layer assumes the linear function  $f(x)=x$ . The input data are the incidence angles ( $\theta$ ) and  $\cos(\Phi-\varphi)$ , and NRCS ( $\sigma$ ), and wind speed (V) while the output data are  $H_{1/3}$  or  $H_{1/3}/(gT^2)$ . In the following equation,

$$A_j = f\left(\sum_{i=1}^d \omega_{ij} x_i\right) \quad j=1, \dots, n.$$

$A_j$  is the output of the  $j$ th neuron,  $d$  is the amount of input, and  $n$  is the neuron amount of the hidden layer. The connection weights are determined during the learning phase using the back-propagation network (Lin et al., 2006).

The retrieved  $H_{1/3}$  and  $H_{1/3}/(gT^2)$  from scatterometer data are compared with the  $H_{1/3}$  and  $H_{1/3}/(gT^2)$  values from buoy data in Figs.4–7 and Table 1.

Table 1  $H_{1/3}$  (m) and  $H_{1/3}/(gT^2)$  RMS for NN inversion

Item	$H_{1/3}$	$H_{1/3}/(gT^2)$
<b>Wind-wave Domination</b>		
Corr1	0.75	0.83
RMS1	0.51 m	0.000 97
Error1	0.41 m	0.000 74
Bias1	-0.002 8 m	1.29e-006
<b>Swell domination</b>		
Corr2	0.84	0.92
RMS2	0.72 m	0.000 77
Error2	0.55 m	0.000 6
Bias2	0.002 m	6.06e-006

In Table 1, Corr is correlation coefficient, RMS for root mean square, and

$$\text{RMS}=\sqrt{\frac{1}{N} \sum_{k=1}^N (\omega_k^1 - \omega_k^2)^2} \quad (1)$$

$$\text{Error}=\frac{1}{N} \sum_{k=1}^N |\omega_k^1 - \omega_k^2| \quad (2)$$

$$\text{Bias}=\frac{1}{N} \sum_{k=1}^N (\omega_k^1 - \omega_k^2) \quad (3)$$

where  $N$  is the number of test data.

## 2.4 Comparison between derived and buoy wave data

If a wave period of buoy is less than 7 s ( $T \leq 7$  s), the case is defined as wind-wave domination. The learning data include 4 100 collocated pairs by random choice. An additional 4 048 ones are randomly taken as test data and not used in the learning phase. Fig.4 shows  $H_{1/3}$  for buoy data in comparison with the retrieved  $H_{1/3}$  from ERS-1/2 scatterometer. Fig.5 compares the  $H_{1/3}/(gT^2)$  from buoy data with the retrieved ones from ERS-1/2 scatterometer. Table 1 displays the detail.

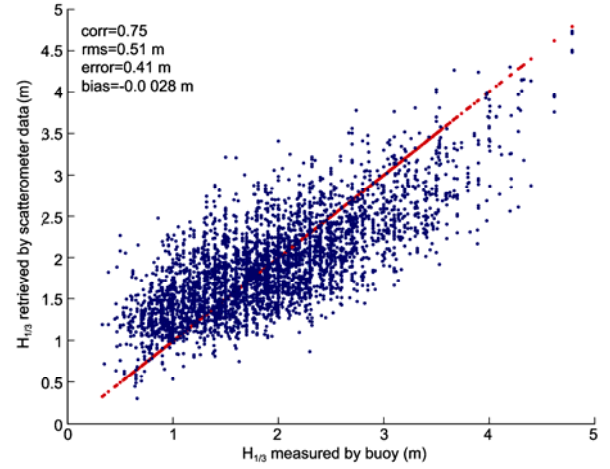


Fig.4 Comparison in  $H_{1/3}$  (m) between buoy data and those retrieved ones from ERS-1/2 scatterometer data

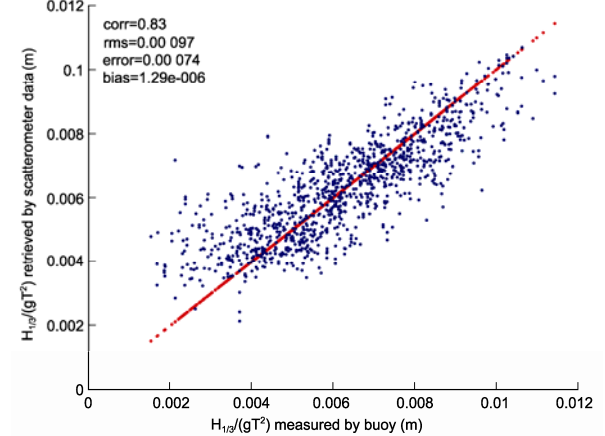
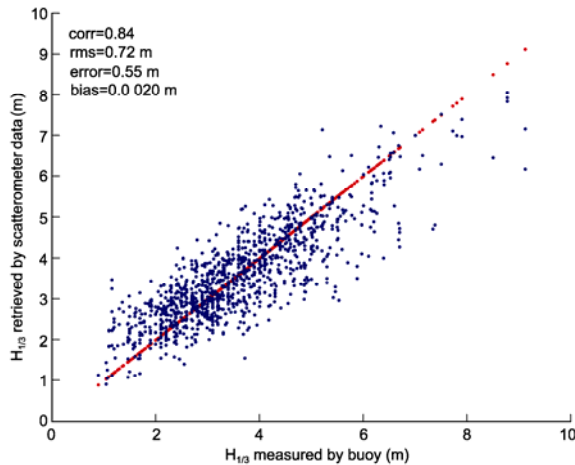


Fig.5 Comparison in  $H_{1/3}/(gT^2)$  between buoy data and retrieved ones from ERS-1/2 scatterometer data

In total, 10 485 the ERS-1/2 scatterometer-yielded data that collocated with NDBC buoy readings are used in this study, of which 8 148 are  $\leq 7$  s and 2 337 are  $> 7$  s in wave period. If a wave period of buoy is  $> 7$  s, swell domination is assumed; otherwise, wind-wave domination. The learning data include 1 200 collocated pairs by random choice. Additional

1 137 collocated pairs are randomly taken as test data and not used in the learning phase. Fig.6 shows the comparison in  $H_{1/3}$  between buoy data and scatterometer data, and Fig.7 is for  $H_{1/3}/(gT^2)$  ones in the same manner.

The bias, average absolute error and root mean square (RMS) of the  $H_{1/3}$  and  $H_{1/3}/(gT^2)$  retrievals with the buoy-measured values are given in Table 1.



**Fig. 6 Comparison in  $H_{1/3}$  between buoy data and retrieved ones that from ERS-1/2 scatterometer data**

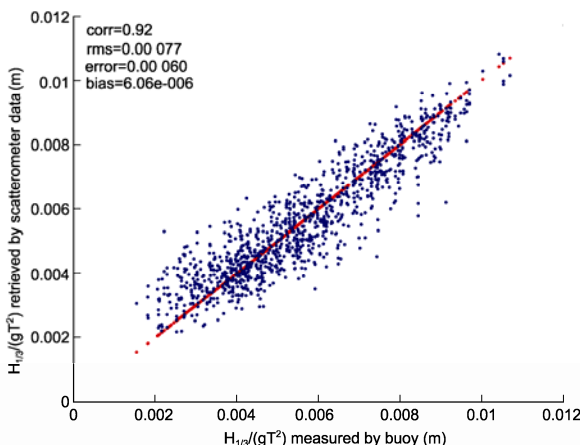


**Fig. 7 The comparison in  $H_{1/3}/(gT^2)$  between the buoys records and those retrieved from ERS-1/2 scatterometer data**

### 3 CONCLUSIONS

A neural networks algorithm is developed by the authors for retrieving  $H_{1/3}$  and  $H_{1/3}/(gT^2)$  (as described in § 2.3) from ERS-1/2 scatterometer data.

In wind-wave domination, the RMS of  $H_{1/3}$  is 0.51 m, while that in swell domination case, 0.72 m. The  $H_{1/3}$  RMS values of the wind-wave domination in this study are consistent with those of Ebuchi and Kawamura's paper (1994), while in the swell domination, the RMS results are on the high end of the Ebuchi and Kawamura (1994) results. It shows that the effect of swell on the radar cross section is significant. It is practical to retrieve  $H_{1/3}$  and  $H_{1/3}/(gT^2)$  values from the ERS-1/2 scatterometer with neural networks methods. In the future, the results from  $H_{1/3}/(gT^2)$  retrievals shall be used to calculate  $T$  and wave lengths.

### References

- Ebuchi, N. and H. Kawamura, 1994. Validation of wind speeds and significant wave heights observed by the TOPEX Altimeter around Japan. *Journal of Oceanography* **50**: 479-487.
- Hwang, P. A., W. J. Teague, G. A. Jacobs and D. W. Wang, 1998. A statistical comparison of wind speed, wave height, and wave period derived from satellite altimeters and ocean buoys in the Gulf of Mexico region. *Journal of Geophys. Res.* **103**(C5): 10 451-10 468.
- Lin, M. S., X. G. Song and X. W. Jiang, 2006. Neural network wind retrieval from ERS-1/2 scatterometer data. *Acta Oceanologica Sinica* **25**(3): 35-39.
- Nghiem, S. V., K. Li, S. H. Lou, G. Neumann, R. E. McIntosh, S. C. Carson, J. R. Carswell, E. J. Walsh, M. A. Donelan, and W. M. Drennan, 1995. Observations of ocean radar backscatter at Ku and C-bands in the presence of large waves during the surface wave dynamics experiment. *IEEE Trans. Geosci. Remote Sens.* **33**(3): 708-721.
- Quilfen, Y. and B. Chapron, 2003. Relationship between ERS Scatterometer Measurement and Integrated Wind and Wave Parameters. *Journal of Atmospheric and Oceanic Technology* **21**: 368-373.
- Stephen L. Durden and John F. Vesey, 1985. A Physical Radar Cross-Section Model for a Wind-Driven Sea with Swell. *IEEE Journal of Oceanic Engineering*. **10**(4): 445-451.
- Tran, N., B. Chapron and D. Vandemark, 2007. Effect of Long Waves on Ku-Band Ocean Radar Backscatter at Low Incidence Angles Using TRMM and Altimeter Data. *IEEE Geosci. & Remote Sensing Lett.* **4**(4): 542-546.